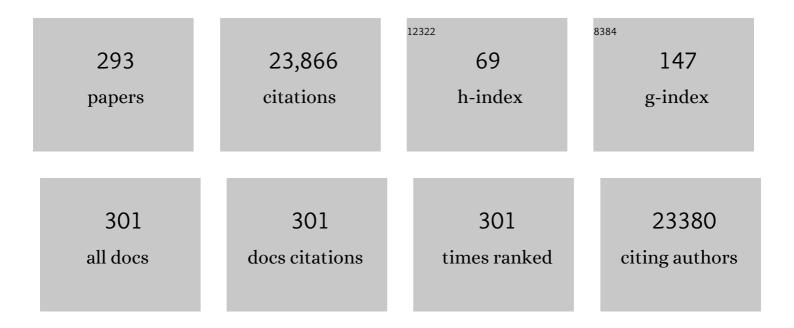
Cheng-Hua Sun

List of Publications by Year in descending order

Source: https://exaly.com/author-pdf/1270972/publications.pdf Version: 2024-02-01



#	Article	IF	CITATIONS
1	Anatase TiO2 single crystals with a large percentage of reactive facets. Nature, 2008, 453, 638-641.	13.7	3,753
2	Unique Electronic Structure Induced High Photoreactivity of Sulfur-Doped Graphitic C ₃ N ₄ . Journal of the American Chemical Society, 2010, 132, 11642-11648.	6.6	1,856
3	Solvothermal Synthesis and Photoreactivity of Anatase TiO ₂ Nanosheets with Dominant {001} Facets. Journal of the American Chemical Society, 2009, 131, 4078-4083.	6.6	1,237
4	Electro-synthesis of ammonia from nitrogen at ambient temperature and pressure in ionic liquids. Energy and Environmental Science, 2017, 10, 2516-2520.	15.6	497
5	Single-Boron Catalysts for Nitrogen Reduction Reaction. Journal of the American Chemical Society, 2019, 141, 2884-2888.	6.6	497
6	Synergistic Effects of B/N Doping on the Visibleâ€Light Photocatalytic Activity of Mesoporous TiO ₂ . Angewandte Chemie - International Edition, 2008, 47, 4516-4520.	7.2	484
7	Stable Hierarchical Bimetal–Organic Nanostructures as HighPerformance Electrocatalysts for the Oxygen Evolution Reaction. Angewandte Chemie - International Edition, 2019, 58, 4227-4231.	7.2	430
8	Nanosized anatase TiO2 single crystals for enhanced photocatalytic activity. Chemical Communications, 2010, 46, 755-757.	2.2	403
9	Promising prospects for 2D d ² –d ⁴ M ₃ C ₂ transition metal carbides (MXenes) in N ₂ capture and conversion into ammonia. Energy and Environmental Science, 2016, 9, 2545-2549.	15.6	395
10	Understanding of Electrochemical Mechanisms for CO ₂ Capture and Conversion into Hydrocarbon Fuels in Transition-Metal Carbides (MXenes). ACS Nano, 2017, 11, 10825-10833.	7.3	359
11	Potassiumâ€Ionâ€Assisted Regeneration of Active Cyano Groups in Carbon Nitride Nanoribbons: Visibleâ€Lightâ€Driven Photocatalytic Nitrogen Reduction. Angewandte Chemie - International Edition, 2019, 58, 16644-16650.	7.2	356
12	Surfactantâ€Assisted Phase‧elective Synthesis of New Cobalt MOFs and Their Efficient Electrocatalytic Hydrogen Evolution Reaction. Angewandte Chemie - International Edition, 2017, 56, 13001-13005.	7.2	334
13	Band-to-Band Visible-Light Photon Excitation and Photoactivity Induced by Homogeneous Nitrogen Doping in Layered Titanates. Chemistry of Materials, 2009, 21, 1266-1274.	3.2	284
14	Efficient metal ion sieving in rectifying subnanochannels enabled by metal–organic frameworks. Nature Materials, 2020, 19, 767-774.	13.3	275
15	Simultaneously Tuning Charge Separation and Oxygen Reduction Pathway on Graphitic Carbon Nitride by Polyethylenimine for Boosted Photocatalytic Hydrogen Peroxide Production. ACS Catalysis, 2020, 10, 3697-3706.	5.5	275
16	Synthesis and Electromagnetic, Microwave Absorbing Properties of Core–Shell Fe ₃ O ₄ –Poly(3, 4-ethylenedioxythiophene) Microspheres. ACS Applied Materials & Interfaces, 2011, 3, 3839-3845.	4.0	265
17	Carbon for the oxygen reduction reaction: a defect mechanism. Journal of Materials Chemistry A, 2015, 3, 11736-11739.	5.2	261
18	Titania-water interactions: a review of theoretical studies. Journal of Materials Chemistry, 2010, 20,	6.7	255

10319.

#	Article	IF	CITATIONS
19	Conversion of dinitrogen to ammonia on Ru atoms supported on boron sheets: a DFT study. Journal of Materials Chemistry A, 2019, 7, 4771-4776.	5.2	251
20	Promoting Oxygen Evolution Reactions through Introduction of Oxygen Vacancies to Benchmark NiFe–OOH Catalysts. ACS Energy Letters, 2018, 3, 1515-1520.	8.8	249
21	Higher charge/discharge rates of lithium-ions across engineered TiO2 surfaces leads to enhanced battery performance. Chemical Communications, 2010, 46, 6129.	2.2	216
22	Three-dimensional porous graphene-like sheets synthesized from biocarbon <i>via</i> low-temperature graphitization for a supercapacitor. Green Chemistry, 2018, 20, 694-700.	4.6	202
23	Lithium Storage on Graphdiyne Predicted by DFT Calculations. Journal of Physical Chemistry C, 2012, 116, 26222-26226.	1.5	198
24	Ultra-thin anatase TiO ₂ nanosheets dominated with {001} facets: thickness-controlled synthesis, growth mechanism and water-splitting properties. CrystEngComm, 2011, 13, 1378-1383.	1.3	189
25	Feasibility of N ₂ Binding and Reduction to Ammonia on Feâ€Đeposited MoS ₂ 2D Sheets: A DFT Study. Chemistry - A European Journal, 2017, 23, 8275-8279.	1.7	173
26	Hydrogenation Synthesis of Blue TiO ₂ for High-Performance Lithium-Ion Batteries. Journal of Physical Chemistry C, 2014, 118, 8824-8830.	1.5	167
27	Combination of nanosizing and interfacial effect: Future perspective for designing Mg-based nanomaterials for hydrogen storage. Renewable and Sustainable Energy Reviews, 2015, 44, 289-303.	8.2	164
28	Computational Study of MoN ₂ Monolayer as Electrochemical Catalysts for Nitrogen Reduction. Journal of Physical Chemistry C, 2017, 121, 27563-27568.	1.5	164
29	Flexible Carbon-Fiber/Semimetal Bi Nanosheet Arrays as Separable and Recyclable Plasmonic Photocatalysts and Photoelectrocatalysts. ACS Applied Materials & Interfaces, 2020, 12, 24845-24854.	4.0	161
30	Hydrothermal Stability of {001} Faceted Anatase TiO ₂ . Chemistry of Materials, 2011, 23, 3486-3494.	3.2	157
31	Lithiumâ€Catalyzed Dehydrogenation of Ammonia Borane within Mesoporous Carbon Framework for Chemical Hydrogen Storage. Advanced Functional Materials, 2009, 19, 265-271.	7.8	156
32	An Aluminum–Sulfur Battery with a Fast Kinetic Response. Angewandte Chemie - International Edition, 2018, 57, 1898-1902.	7.2	154
33	Rational Design of Hydroxylâ€Rich Ti ₃ C ₂ T _x MXene Quantum Dots for Highâ€Performance Electrochemical N ₂ Reduction. Advanced Energy Materials, 2020, 10, 2000797.	10.2	153
34	Confined Fe–Cu Clusters as Subâ€Nanometer Reactors for Efficiently Regulating the Electrochemical Nitrogen Reduction Reaction. Advanced Materials, 2020, 32, e2004382.	11.1	152
35	Graphene oxide: An emerging electromaterial for energy storage and conversion. Journal of Energy Chemistry, 2021, 55, 323-344.	7.1	146
36	Fabrication of three-dimensional ZnO/TiO2 heteroarchitectures via a solution process. Journal of Materials Chemistry, 2008, 18, 3909.	6.7	145

#	Article	IF	CITATIONS
37	Research progress and materials selection guidelines on mixed conducting perovskite-type ceramic membranes for oxygen production. RSC Advances, 2011, 1, 1661.	1.7	143
38	Hierarchical Structures of Singleâ€Crystalline Anatase TiO ₂ Nanosheets Dominated by {001} Facets. Chemistry - A European Journal, 2011, 17, 1423-1427.	1.7	143
39	Activation of Photocatalytic Water Oxidation on N-Doped ZnO Bundle-like Nanoparticles under Visible Light. Journal of Physical Chemistry C, 2013, 117, 4937-4942.	1.5	143
40	Nâ€Doped CsTaWO ₆ as a New Photocatalyst for Hydrogen Production from Water Splitting Under Solar Irradiation. Advanced Functional Materials, 2011, 21, 126-132.	7.8	135
41	Subâ€2 nm Thiophosphate Nanosheets with Heteroatom Doping for Enhanced Oxygen Electrocatalysis. Advanced Functional Materials, 2021, 31, 2100618.	7.8	133
42	lodine doped anatase TiO2 photocatalyst with ultra-long visible light response: correlation between geometric/electronic structures and mechanisms. Journal of Materials Chemistry, 2009, 19, 2822.	6.7	127
43	A DFT study of planar vs. corrugated graphene-like carbon nitride (g-C ₃ N ₄) and its role in the catalytic performance of CO ₂ conversion. Physical Chemistry Chemical Physics, 2016, 18, 18507-18514.	1.3	125
44	Novel 1D carbon nanotubes uniformly wrapped nanoscale MgH2 for efficient hydrogen storage cycling performances with extreme high gravimetric and volumetric capacities. Nano Energy, 2019, 61, 540-549.	8.2	124
45	Amorphous Boron Carbide on Titanium Dioxide Nanobelt Arrays for Highâ€Efficiency Electrocatalytic NO Reduction to NH ₃ . Angewandte Chemie - International Edition, 2022, 61, .	7.2	121
46	Long lifetime photoluminescence in N, S co-doped carbon quantum dots from an ionic liquid and their applications in ultrasensitive detection of pesticides. Carbon, 2016, 104, 33-39.	5.4	117
47	Importance of Oxygen in the Metal-Free Catalytic Growth of Single-Walled Carbon Nanotubes from SiO _{<i>x</i>} by a Vaporâ^'Solidâ^'Solid Mechanism. Journal of the American Chemical Society, 2011, 133, 197-199.	6.6	116
48	Efficient Promotion of Anatase TiO2 Photocatalysis via Bifunctional Surface-Terminating Tiâ^'Oâ^'Bâ^'N Structures. Journal of Physical Chemistry C, 2009, 113, 12317-12324.	1.5	115
49	Sulfur doped anatase TiO2 single crystals with a high percentage of {0 0 1} facets. Journal of Colloid and Interface Science, 2010, 349, 477-483.	5.0	112
50	A Ta-TaS2 monolith catalyst with robust and metallic interface for superior hydrogen evolution. Nature Communications, 2021, 12, 6051.	5.8	112
51	Real-Time Observation of Reconstruction Dynamics on TiO ₂ (001) Surface under Oxygen via an Environmental Transmission Electron Microscope. Nano Letters, 2016, 16, 132-137.	4.5	109
52	Proposing the prospects of Ti ₃ CN transition metal carbides (MXenes) as anodes of Li-ion batteries: a DFT study. Physical Chemistry Chemical Physics, 2016, 18, 32937-32943.	1.3	105
53	AlN nanoparticle-reinforced nanocrystalline Al matrix composites: Fabrication and mechanical properties. Materials Science & Engineering A: Structural Materials: Properties, Microstructure and Processing, 2009, 505, 151-156.	2.6	103
54	Nitrogen-doped titania nanosheets towards visible light response. Chemical Communications, 2009, , 1383.	2.2	95

#	Article	IF	CITATIONS
55	Hydrogen Incorporation and Storage in Well-Defined Nanocrystals of Anatase Titanium Dioxide. Journal of Physical Chemistry C, 2011, 115, 25590-25594.	1.5	93
56	Two-dimensional g-C3N4/TiO2 nanocomposites as vertical Z-scheme heterojunction for improved photocatalytic water disinfection. Catalysis Today, 2019, 335, 243-251.	2.2	93
57	Theoretical Evaluation of Possible 2D Boron Monolayer in N ₂ Electrochemical Conversion into Ammonia. Journal of Physical Chemistry C, 2018, 122, 25268-25273.	1.5	91
58	A synergistic effect between S-scheme heterojunction and Noble-metal free cocatalyst to promote the hydrogen evolution of ZnO/CdS/MoS2 photocatalyst. Chemical Engineering Journal, 2021, 424, 130368.	6.6	90
59	Enhanced sorption of trivalent antimony by chitosan-loaded biochar in aqueous solutions: Characterization, performance and mechanisms. Journal of Hazardous Materials, 2022, 425, 127971.	6.5	89
60	Photocatalytic Hydrogen Production from Water Using N-Doped Ba ₅ Ta ₄ O ₁₅ under Solar Irradiation. Journal of Physical Chemistry C, 2011, 115, 15674-15678.	1.5	88
61	Functional anion concept: effect of fluorine anion on hydrogen storage of sodium alanate. Physical Chemistry Chemical Physics, 2007, 9, 1499-1502.	1.3	83
62	Inâ€Situ Observation of Hydrogenâ€Induced Surface Faceting for Palladium–Copper Nanocrystals at Atmospheric Pressure. Angewandte Chemie - International Edition, 2016, 55, 12427-12430.	7.2	81
63	Destabilization of Mg–H bonding through nano-interfacial confinement by unsaturated carbon for hydrogen desorption from MgH2. Physical Chemistry Chemical Physics, 2013, 15, 5814.	1.3	80
64	Theoretical Investigation of Single and Double Transition Metals Anchored on Graphyne Monolayer for Nitrogen Reduction Reaction. Journal of Physical Chemistry C, 2020, 124, 15295-15301.	1.5	79
65	Tuning the Hydrogen Evolution Performance of Metallic 2D Tantalum Disulfide by Interfacial Engineering. ACS Nano, 2019, 13, 11874-11881.	7.3	77
66	Growth Velocity and Direct Length-Sorted Growth of Short Single-Walled Carbon Nanotubes by a Metal-Catalyst-Free Chemical Vapor Deposition Process. ACS Nano, 2009, 3, 3421-3430.	7.3	76
67	The examination of graphene oxide for rechargeable lithium storage as a novel cathode material. Journal of Materials Chemistry A, 2013, 1, 3607.	5.2	73
68	Preparation of self-supporting hierarchical nanostructured anatase/rutile composite TiO2 film. Chemical Communications, 2008, , 3293.	2.2	72
69	Oxygen vacancies for promoting the electrochemical nitrogen reduction reaction. Journal of Materials Chemistry A, 2021, 9, 6694-6709.	5.2	71
70	Sulfated Carbon Quantum Dots as Efficient Visibleâ€Light Switchable Acid Catalysts for Roomâ€Temperature Ringâ€Opening Reactions. Angewandte Chemie - International Edition, 2015, 54, 8420-8424.	7.2	68
71	Design strategies of two-dimensional metal–organic frameworks toward efficient electrocatalysts for N ₂ reduction: cooperativity of transition metals and organic linkers. Nanoscale, 2021, 13, 19247-19254.	2.8	67
72	Preparation of new sulfur-doped and sulfur/nitrogen co-doped CsTaWO6 photocatalysts for hydrogen production from water under visible light. Journal of Materials Chemistry, 2011, 21, 8871.	6.7	66

#	Article	IF	CITATIONS
73	Metallic Ni nanocatalyst in situ formed from a metal–organic-framework by mechanochemical reaction for hydrogen storage in magnesium. Journal of Materials Chemistry A, 2015, 3, 8294-8299.	5.2	65
74	An oxalate cathode for lithium ion batteries with combined cationic and polyanionic redox. Nature Communications, 2019, 10, 3483.	5.8	65
75	Electronic Coupling and Catalytic Effect on H2 Evolution of MoS2/Graphene Nanocatalyst. Scientific Reports, 2014, 4, 6256.	1.6	64
76	Two-Dimensional Boron Sheets as Metal-Free Catalysts for Hydrogen Evolution Reaction. Journal of Physical Chemistry C, 2018, 122, 19051-19055.	1.5	63
77	Computational Design of Single-Molybdenum Catalysts for the Nitrogen Reduction Reaction. Journal of Physical Chemistry C, 2019, 123, 2347-2352.	1.5	63
78	Double transition metal atoms anchored on Graphdiyne as promising catalyst for electrochemical nitrogen reduction reaction. Journal of Materials Science and Technology, 2021, 77, 244-251.	5.6	63
79	Van der Waals interactions between two parallel infinitely long single-walled nanotubes. Chemical Physics Letters, 2005, 403, 343-346.	1.2	62
80	In situ polymerization and characterization of grafted poly (3,4-ethylenedioxythiophene)/multiwalled carbon nanotubes composite with high electrochemical performances. Electrochimica Acta, 2013, 87, 394-400.	2.6	61
81	Nitrogen doping in ion-exchangeable layered tantalate towards visible-light induced water oxidation. Chemical Communications, 2011, 47, 6293.	2.2	59
82	Blue hydrogenated lithium titanate as a high-rate anode material for lithium-ion batteries. Journal of Materials Chemistry A, 2014, 2, 6353.	5.2	58
83	Surfactantâ€Assisted Phase‣elective Synthesis of New Cobalt MOFs and Their Efficient Electrocatalytic Hydrogen Evolution Reaction. Angewandte Chemie, 2017, 129, 13181-13185.	1.6	58
84	Nitrogenase-Inspired Atomically Dispersed Fe–S–C Linkages for Improved Electrochemical Reduction of Dinitrogen to Ammonia. ACS Catalysis, 2022, 12, 1443-1451.	5.5	58
85	Capacity-controllable Li-rich cathode materials for lithium-ion batteries. Nano Energy, 2014, 6, 92-102.	8.2	53
86	Ultraselective Monovalent Metal Ion Conduction in a Three-Dimensional Sub-1 nm Nanofluidic Device Constructed by Metal–Organic Frameworks. ACS Nano, 2021, 15, 1240-1249.	7.3	52
87	Strong Interaction between Gold and Anatase TiO ₂ (001) Predicted by First Principle Studies. Journal of Physical Chemistry C, 2012, 116, 3524-3531.	1.5	50
88	Exploration of iron borides as electrochemical catalysts for the nitrogen reduction reaction. Journal of Materials Chemistry A, 2019, 7, 21507-21513.	5.2	49
89	Transition-metal-doped Fe2O3 nanoparticles for oxygen evolution reaction. Progress in Natural Science: Materials International, 2018, 28, 430-436.	1.8	48
90	Axial Young's modulus prediction of single-walled carbon nanotube arrays with diameters from nanometer to meter scales. Applied Physics Letters, 2005, 87, 193101.	1.5	47

#	Article	IF	CITATIONS
91	Field Emission and Cathodoluminescence of ZnS Hexagonal Pyramids of Zinc Blende Structured Single Crystals. Advanced Functional Materials, 2009, 19, 484-490.	7.8	47
92	An <i>in situ</i> assembled WO ₃ –TiO ₂ vertical heterojunction for enhanced Z-scheme photocatalytic activity. Nanoscale, 2020, 12, 8775-8784.	2.8	47
93	Lattice Distortion Oriented Angular Self-Assembly of Monolayer Titania Sheets. Journal of the American Chemical Society, 2011, 133, 695-697.	6.6	46
94	Step-wise controlled growth of metal@TiO ₂ core–shells with plasmonic hot spots and their photocatalytic properties. Journal of Materials Chemistry A, 2014, 2, 12776.	5.2	45
95	An NIR-sensitive layered supramolecular nanovehicle for combined dual-modal imaging and synergistic therapy. Nanoscale, 2017, 9, 10367-10374.	2.8	45
96	Constructing a Metallic/Semiconducting TaB ₂ /Ta ₂ O ₅ Core/Shell Heterostructure for Photocatalytic Hydrogen Evolution. Advanced Energy Materials, 2014, 4, 1400057.	10.2	44
97	Atomic-Scale Observation of Vapor–Solid Nanowire Growth <i>via</i> Oscillatory Mass Transport. ACS Nano, 2016, 10, 763-769.	7.3	43
98	An Aluminum–Sulfur Battery with a Fast Kinetic Response. Angewandte Chemie, 2018, 130, 1916-1920.	1.6	43
99	Titania polymorphs derived from crystalline titanium diboride. CrystEngComm, 2009, 11, 2677.	1.3	42
100	Electropolymerized poly(3,4-ethylenedioxythiophene):poly(styrene sulfonate) (PEDOT:PSS) film on ITO glass and its application in photovoltaic device. Solar Energy Materials and Solar Cells, 2010, 94, 390-394.	3.0	42
101	Self-Assembly and Cathodoluminescence of Microbelts from Cu-Doped Boron Nitride Nanotubes. ACS Nano, 2008, 2, 1523-1532.	7.3	41
102	Enhanced catalytic effect of TiO2@rGO synthesized by one-pot ethylene glycol-assisted solvothermal method for MgH2. Journal of Alloys and Compounds, 2021, 881, 160644.	2.8	41
103	4- <i>tert</i> -Butyl Pyridine Bond Site and Band Bending on TiO ₂ (110). Journal of Physical Chemistry C, 2010, 114, 2315-2320.	1.5	40
104	In Situ STEM Determination of the Atomic Structure and Reconstruction Mechanism of the TiO ₂ (001) (1 × 4) Surface. Chemistry of Materials, 2017, 29, 3189-3194.	3.2	40
105	Lowâ€Valence Metal Single Atoms on Graphdiyne Promotes Electrochemical Nitrogen Reduction via Mâ€ŧoâ€N ₂ Ï€â€Backdonation. Advanced Functional Materials, 2022, 32, .	7.8	38
106	New Insight into the Interaction between Propylene Carbonate-Based Electrolytes and Graphite Anode Material for Lithium Ion Batteries. Journal of Physical Chemistry C, 2007, 111, 4740-4748.	1.5	37
107	A formation mechanism of oxygen vacancies in a MnO2 monolayer: a DFT + U study. Physical Chemistry Chemical Physics, 2011, 13, 11325.	1.3	37
108	Efficient Visible Light Driven Ammonia Synthesis on Sandwich Structured C3N4/MoS2/Mn3O4 catalyst. Applied Catalysis B: Environmental, 2021, 281, 119476.	10.8	37

#	Article	IF	CITATIONS
109	Synthesis and microwave absorbing properties of poly(3,4â€ethylenedioxythiophene) (PEDOT) microspheres. Polymers for Advanced Technologies, 2011, 22, 532-537.	1.6	36
110	Enhanced hydrogen desorption properties of magnesium hydride by coupling non-metal doping and nano-confinement. Applied Physics Letters, 2015, 107, .	1.5	36
111	Stable Hierarchical Bimetal–Organic Nanostructures as HighPerformance Electrocatalysts for the Oxygen Evolution Reaction. Angewandte Chemie, 2019, 131, 4271-4275.	1.6	36
112	The Role of Atomic Vacancy on Water Dissociation over Titanium Dioxide Nanosheet: A Density Functional Theory Study. Journal of Physical Chemistry C, 2012, 116, 2477-2482.	1.5	35
113	One-pot scalable synthesis of all-inorganic perovskite nanocrystals with tunable morphology, composition and photoluminescence. CrystEngComm, 2017, 19, 7041-7049.	1.3	35
114	In situ synthesis of PtPd bimetallic nanocatalysts supported on graphene nanosheets for methanol oxidation using triblock copolymer as reducer and stabilizer. Journal of Electroanalytical Chemistry, 2016, 783, 132-139.	1.9	34
115	Confinement of carbon dots localizing to the ultrathin layered double hydroxides toward simultaneous triple-mode bioimaging and photothermal therapy. Talanta, 2018, 184, 50-57.	2.9	34
116	Computational Investigation of MgH ₂ /Graphene Heterojunctions for Hydrogen Storage. Journal of Physical Chemistry C, 2021, 125, 2357-2363.	1.5	33
117	Synergistic effects of heteroatom-decorated MXene catalysts for CO reduction reactions. Nanoscale, 2020, 12, 15880-15887.	2.8	32
118	Controlled fabrication of highly conductive three-dimensional flowerlike poly (3,4-ethylenedioxythiophene) nanostructures. Journal of Materials Chemistry, 2011, 21, 7123.	6.7	31
119	A new crystal: layer-structured rhombohedral In3Se4. CrystEngComm, 2014, 16, 393-398.	1.3	31
120	A Terbiumâ€Organic Framework Material for Highly Sensitive Sensing of Fe ³⁺ in Aqueous and Biological Systems: Experimental Studies and Theoretical Analysis. ChemistrySelect, 2016, 1, 3555-3561.	0.7	31
121	Nanoscale Behavior and Manipulation of the Phase Transition in Singleâ€Crystal Cu ₂ Se. Advanced Materials, 2019, 31, e1804919.	11.1	31
122	Insights into the efficient charge separation over Nb2O5/2D-C3N4 heterostructure for exceptional visible-light driven H2 evolution. Journal of Energy Chemistry, 2022, 65, 548-555.	7.1	31
123	Microwave absorbing properties of Fe ₃ O ₄ –poly(3, 4â€ethylenedioxythiophene) hybrids in lowâ€frequency band. Polymers for Advanced Technologies, 2014, 25, 83-88.	1.6	30
124	Purification of Multiwalled Carbon Nanotubes by Annealing and Extraction Based on the Difference in van der Waals Potential. Journal of Physical Chemistry B, 2006, 110, 9477-9481.	1.2	29
125	A facile process to produce highly conductive poly(3,4-ethylenedioxythiophene) films for ITO-free flexible OLED devices. Journal of Materials Chemistry C, 2014, 2, 916-924.	2.7	29
126	Free-standing ternary PtPdRu nanocatalysts with enhanced activity and durability for methanol electrooxidation. Electrochimica Acta, 2016, 222, 1094-1102.	2.6	29

#	Article	IF	CITATIONS
127	Bandgap narrowing of titanium oxide nanosheets: homogeneous doping of molecular iodine for improved photoreactivity. Journal of Materials Chemistry, 2011, 21, 14672.	6.7	28
128	Effects of the Particle Size of BaTiO3 Fillers on Fabrication and Dielectric Properties of BaTiO3/Polymer/Al Films for Capacitor Energy-Storage Application. Materials, 2019, 12, 439.	1.3	28
129	Electrocatalytic Nitrogen Reduction by Transition Metal Single-Atom Catalysts on Polymeric Carbon Nitride. Journal of Physical Chemistry C, 2021, 125, 13880-13888.	1.5	28
130	Single-Iron Supported on Defective Graphene as Efficient Catalysts for Oxygen Reduction Reaction. Journal of Physical Chemistry C, 2020, 124, 13283-13290.	1.5	28
131	Simple approach to estimating the van der Waals interaction between carbon nanotubes. Physical Review B, 2006, 73, .	1.1	27
132	The role of V2O5 on the dehydrogenation and hydrogenation in magnesium hydride: An <i>ab initio</i> study. Applied Physics Letters, 2008, 92, .	1.5	27
133	Impact of H-termination on the nitrogen reduction reaction of molybdenum carbide as an electrochemical catalyst. Physical Chemistry Chemical Physics, 2018, 20, 23338-23343.	1.3	27
134	Hydrogen-Rich 2D Halide Perovskite Scintillators for Fast Neutron Radiography. Journal of the American Chemical Society, 2021, 143, 21302-21311.	6.6	27
135	Understanding the Influence of Lattice Composition on the Photocatalytic Activity of Defectâ€Pyrochloreâ€6tructured Semiconductor Mixed Oxides. Advanced Functional Materials, 2015, 25, 905-912.	7.8	26
136	Potassiumâ€lonâ€Assisted Regeneration of Active Cyano Groups in Carbon Nitride Nanoribbons: Visibleâ€Lightâ€Driven Photocatalytic Nitrogen Reduction. Angewandte Chemie, 2019, 131, 16797-16803.	1.6	26
137	Inhomogeneous charge transfer within monolayer zinc phthalocyanine absorbed on TiO2(110). Journal of Chemical Physics, 2012, 136, 154703.	1.2	25
138	Ti0.89Si0.11O2 single crystals bound by high-index {201} facets showing enhanced visible-light photocatalytic hydrogen evolution. Chemical Communications, 2013, 49, 2016.	2.2	25
139	Origin of the Visible Light Absorption of Boron/Nitrogen Co-doped Anatase TiO ₂ . Journal of Physical Chemistry C, 2013, 117, 26454-26459.	1.5	25
140	Ni-induced stepwise capacity increase in Ni-poor Li-rich cathode materials for high performance lithium ion batteries. Nano Research, 2015, 8, 808-820.	5.8	25
141	Vertically-heterostructured TiO2-Ag-rGO ternary nanocomposite constructed with {001} facetted TiO2 nanosheets for enhanced Pt-free hydrogen production. International Journal of Hydrogen Energy, 2018, 43, 1508-1515.	3.8	25
142	In Operando Identification of In Situ Formed Metalloid Zinc ^{δ+} Active Sites for Highly Efficient Electrocatalyzed Carbon Dioxide Reduction. Angewandte Chemie - International Edition, 2022, 61, .	7.2	25
143	AlN nanowires for Al-based composites with high strength and low thermal expansion. Journal of Materials Research, 2007, 22, 2711-2718.	1.2	24
144	Oxygen vacancy induced structural variations of exfoliated monolayerMnO2sheets. Physical Review B, 2010, 81, .	1.1	24

#	Article	IF	CITATIONS
145	Rational Design of Graphene-Supported Single-Atom Catalysts for Electroreduction of Nitrogen. Inorganic Chemistry, 2021, 60, 18314-18324.	1.9	24
146	Nanostructural instability of single-walled carbon nanotubes during electron beam induced shrinkage. Carbon, 2011, 49, 3120-3124.	5.4	23
147	Recovery of rare earth elements from waste fluorescent phosphors: Na2O2 molten salt decomposition. Journal of Material Cycles and Waste Management, 2014, 16, 635-641.	1.6	23
148	Experimental and theoretical study of the oxidation of ventilation air methane over Fe ₂ O ₃ and CuO. Physical Chemistry Chemical Physics, 2015, 17, 16277-16284.	1.3	23
149	An intensified π-hole in beryllium-doped boron nitride meshes: its determinant role in CO2 conversion into hydrocarbon fuels. Chemical Communications, 2016, 52, 3548-3551.	2.2	23
150	A simple and recyclable molten-salt route to prepare superthin biocarbon sheets based on the high water-absorbent agaric for efficient lithium storage. Carbon, 2020, 157, 286-294.	5.4	23
151	Water as a cocatalyst for photocatalytic H2 production from formic acid. Nano Today, 2020, 35, 100968.	6.2	23
152	The effect of Fe doping on adsorption of CO ₂ /N ₂ within carbon nanotubes: a density functional theory study with dispersion corrections. Nanotechnology, 2009, 20, 375701.	1.3	22
153	Charge carrier exchange at chemically modified graphene edges: a density functional theory study. Journal of Materials Chemistry, 2012, 22, 8321.	6.7	22
154	How to achieve maximum charge carrier loading on heteroatom-substituted graphene nanoribbon edges: density functional theory study. Journal of Materials Chemistry, 2012, 22, 13751.	6.7	22
155	Chemically modified ribbon edge stimulated H2 dissociation: a first-principles computational study. Physical Chemistry Chemical Physics, 2013, 15, 8054.	1.3	22
156	Direct observation of Pt nanocrystal coalescence induced by electron-excitation-enhanced van der Waals interactions. Nano Research, 2014, 7, 308-314.	5.8	22
157	Oxygen permeability and CO2-tolerance of Ce0.9Gd0.1O2â^î´â€" SrCo0.8Fe0.1Nb0.1O3â^î´ dual-phase membrane. Journal of Alloys and Compounds, 2015, 646, 204-210.	2.8	22
158	Adsorption and dissociation behavior of water on pristine and defected calcite {1 0 4} surfaces: A DFT study. Applied Surface Science, 2021, 556, 149777.	3.1	22
159	Surface fractal dimension of single-walled carbon nanotubes. Physical Review B, 2004, 69, .	1.1	21
160	Interaction of Water with the Fluorine-Covered Anatase TiO ₂ (001) Surface. Journal of Physical Chemistry C, 2011, 115, 17092-17096.	1.5	21
161	3D flowerlike poly(3,4-ethylenedioxythiophene) for high electrochemical capacitive energy storage. Electrochimica Acta, 2013, 106, 219-225.	2.6	21
162	Rapid and sensitive biomarker detection using molecular imprinting polymer hydrogel and surface-enhanced Raman scattering. Royal Society Open Science, 2018, 5, 171488.	1.1	21

#	Article	IF	CITATIONS
163	Inâ€Situ Observation of Hydrogenâ€Induced Surface Faceting for Palladium–Copper Nanocrystals at Atmospheric Pressure. Angewandte Chemie, 2016, 128, 12615-12618.	1.6	20
164	Unraveling the Role of Ligands in the Hydrogen Evolution Mechanism Catalyzed by [NiFe] Hydrogenases. ACS Catalysis, 2016, 6, 5541-5548.	5.5	20
165	Enhancing hydrogen evolution of MoS2 basal planes by combining single-boron catalyst and compressive strain. Frontiers of Physics, 2020, 15, 1.	2.4	20
166	Ultrathin α-Mo2C dominated by (100) Surface/Cu Schottky junction as efficient catalyst for hydrogen evolution. International Journal of Hydrogen Energy, 2019, 44, 853-859.	3.8	19
167	TM3 (TMÂ=ÂV, Fe, Mo, W) single-cluster catalyst confined on porous BN for electrocatalytic nitrogen reduction. Journal of Materials Science and Technology, 2022, 108, 46-53.	5.6	19
168	Selected absorption behavior of sulfur on single-walled carbon nanotubes by DFT. Chemical Physics Letters, 2008, 454, 305-309.	1.2	18
169	Density functional theory study on adsorption of Pt nanoparticle on graphene. International Journal of Hydrogen Energy, 2013, 38, 6283-6287.	3.8	18
170	Enhancement of hydrogen storage properties by in situ formed LaH3 and Mg2NiH4 during milling MgH2 with porous LaNiO3. Catalysis Today, 2018, 318, 113-118.	2.2	18
171	Dual-ion battery with MoS2 cathode. Energy Storage Materials, 2020, 32, 159-166.	9.5	18
172	Electrocatalytic Nitrogen Reduction Performance of Siâ€doped 2D Nanosheets of Boron Nitride Evaluated via Density Functional Theory. ChemCatChem, 2021, 13, 1239-1245.	1.8	18
173	Defective Fe ₃ GeTe ₂ monolayer as a promising electrocatalyst for spontaneous nitrogen reduction reaction. Journal of Materials Chemistry A, 2021, 9, 6945-6954.	5.2	18
174	Stability of Supershort Single-Walled Carbon Nanotubes. Journal of Physical Chemistry B, 2005, 109, 12406-12409.	1.2	17
175	Metal link: A strategy to combine graphene and titanium dioxide for enhanced hydrogen production. International Journal of Hydrogen Energy, 2016, 41, 22034-22042.	3.8	17
176	Exploration of TiO2 as substrates for single metal catalysts: A DFT study. Applied Surface Science, 2020, 533, 147362.	3.1	17
177	Electrocatalytic dinitrogen reduction reaction on silicon carbide: a density functional theory study. Physical Chemistry Chemical Physics, 2020, 22, 21761-21767.	1.3	17
178	Mechanistic Insights into Direct Methane Oxidation to Methanol on Single-Atom Transition-Metal-Modified Graphyne. ACS Applied Nano Materials, 2021, 4, 12006-12016.	2.4	17
179	In situ TEM observation of dissolution and regrowth dynamics of MoO2 nanowires under oxygen. Nano Research, 2017, 10, 397-404.	5.8	16
180	Unveiling the Atomic Structures of the Minority Surfaces of TiO ₂ Nanocrystals. Chemistry of Materials, 2018, 30, 288-295.	3.2	16

#	Article	IF	CITATIONS
181	Unique Layerâ€Dopingâ€Induced Regulation of Charge Behavior in Metalâ€Free Carbon Nitride Photoanodes for Enhanced Performance. ChemSusChem, 2020, 13, 328-333.	3.6	16
182	Trends in C–O and N–O bond scission on rutile oxides described using oxygen vacancy formation energies. Chemical Science, 2020, 11, 4119-4124.	3.7	16
183	Hydrogen bonding effect between active site and protein environment on catalysis performance in H ₂ -producing [NiFe] hydrogenases. Physical Chemistry Chemical Physics, 2018, 20, 6735-6743.	1.3	15
184	First principles study of single Fe atom supported on TiO2(0 0 1) for nitrogen reduction to ammonia. Applied Surface Science, 2022, 572, 151417.	3.1	15
185	Nitrateâ€ŧoâ€Ammonia Conversion on Ru/Ni Hydroxide Hybrid through Zincâ€Nitrate Fuel Cell. Small, 2022, 18, e2200436.	5.2	15
186	Insights into simultaneous adsorption and oxidation of antimonite [Sb(III)] by crawfish shell-derived biochar: spectroscopic investigation and theoretical calculations. Biochar, 2022, 4, .	6.2	15
187	Hydrothermal Synthesis of Nanoporous NiO Rods Self-Supported on Ni Foam as Efficient Electrocatalysts for Hydrogen Evolution Reaction. Jom, 2019, 71, 621-625.	0.9	14
188	BiVO4/TiO2 heterojunction with rich oxygen vacancies for enhanced electrocatalytic nitrogen reduction reaction. Frontiers of Physics, 2021, 16, 1.	2.4	14
189	Nonplanar Distortions and Strain Energies of Polycyclic Aromatic Hydrocarbons. Journal of Physical Chemistry B, 2006, 110, 4563-4568.	1.2	13
190	Facile route to controlled iron oxides/poly(3,4-ethylenedioxythiophene) nanocomposites and microwave absorbing properties. Composites Science and Technology, 2013, 87, 14-21.	3.8	13
191	Site-dependent charge transfer at the Pt(111)-ZnPc interface and the effect of iodine. Journal of Chemical Physics, 2014, 140, 174702.	1.2	13
192	Mechanistic studies of the photo-electrochemical hydrogen evolution reaction on poly(2,2′-bithiophene). Catalysis Science and Technology, 2016, 6, 3253-3262.	2.1	13
193	TiO2-Seeded Hydrothermal Growth of Spherical BaTiO3 Nanocrystals for Capacitor Energy-Storage Application. Crystals, 2020, 10, 202.	1.0	13
194	Selective oxidation of methane to methanol using AuPd@ZIF-8. Catalysis Communications, 2021, 158, 106338.	1.6	13
195	High-Throughput computational screening of Single-atom embedded in defective BN nanotube for electrocatalytic nitrogen fixation. Applied Surface Science, 2022, 591, 153130.	3.1	13
196	Computational study of methyl derivatives of ammonia borane for hydrogen storage. Physical Chemistry Chemical Physics, 2008, 10, 6104.	1.3	12
197	Structure-Dependent 4-Tert-Butyl Pyridine-Induced Band Bending at Ti <mml:math xmlns:mml="http://www.w3.org/1998/Math/MathML"><mml:mrow><mml:msub><mml:mtext>O</mml:mtext>< International Journal of Photoenergy, 2011, 2011, 1-6.</mml:msub></mml:mrow></mml:math 	cmm4mtext	:> 2 2/mml:mi
198	Why is a proton transformed into a hydride by [NiFe] hydrogenases? An intrinsic reactivity analysis based on conceptual DET_Physical Chemistry Chemical Physics 2016, 18, 15369-15374	1.3	12

#	Article	IF	CITATIONS
199	Morphology-Controlled Synthesis of Co3O4 Materials and its Electrochemical Catalytic Properties Towards Oxygen Evolution Reaction. Catalysis Letters, 2018, 148, 3771-3778.	1.4	12
200	Improved catalytic combustion of methane using CuO nanobelts with predominantly (001) surfaces. Beilstein Journal of Nanotechnology, 2018, 9, 2526-2532.	1.5	12
201	Hybrid Amorphous/Crystalline FeNi (Oxy) Hydroxide Nanosheets for Enhanced Oxygen Evolution. ChemCatChem, 2019, 11, 3004-3009.	1.8	12
202	Interlayered MoS2/rGO thin film for efficient lithium storage produced by electrospray deposition and far-infrared reduction. Applied Surface Science, 2020, 499, 143940.	3.1	12
203	Near zero-waste biofuel production from bioderived polyhydroxybutyrate. Fuel, 2021, 286, 119405.	3.4	12
204	p-Block element-doped silicon nanowires for nitrogen reduction reaction: a DFT study. Nanoscale, 2021, 13, 14935-14944.	2.8	12
205	A DFT study of Ti3C2O2 MXenes quantum dots supported on single layer graphene: Electronic structure an hydrogen evolution performance. Frontiers of Physics, 2021, 16, 1.	2.4	12
206	Bridge sulfur vacancies in MoS2 catalyst for reverse water gas shift: A first-principles study. Applied Surface Science, 2021, 561, 149925.	3.1	12
207	Crystallization-Induced Charge-Transfer Change in TiOPc Thin Films Revealed by Resonant Photoemission Spectroscopy. Journal of Physical Chemistry C, 2011, 115, 14969-14977.	1.5	11
208	Structural stability and oxygen permeability of BaCo1â~'Nb O3â~' ceramic membranes for air separation. Journal of Alloys and Compounds, 2015, 638, 38-43.	2.8	11
209	SiS nanosheets as a promising anode material for Li-ion batteries: a computational study. Physical Chemistry Chemical Physics, 2017, 19, 8563-8567.	1.3	11
210	Experimental and Computational Investigation of the Optical, Electronic, and Electrochemical Properties of Hydrogenated α-Fe ₂ O ₃ . Journal of Physical Chemistry C, 2017, 121, 16059-16065.	1.5	11
211	Hierarchically Ordered Nanochannel Array Membrane Reactor with Three-Dimensional Electrocatalytic Interfaces for Electrohydrogenation of CO ₂ to Alcohol. ACS Energy Letters, 2018, 3, 2649-2655.	8.8	11
212	Single PdO loaded on boron nanosheet for methane oxidation: A DFT study. Progress in Natural Science: Materials International, 2019, 29, 367-369.	1.8	11
213	Selectively encapsulating Ag nanoparticles on the surface of two-dimensional graphene for surface-enhanced Raman scattering. Applied Surface Science, 2019, 492, 108-115.	3.1	11
214	Catalytic reduction of carbon dioxide over two-dimensional boron monolayer. Journal of Materials Science and Technology, 2022, 110, 96-102.	5.6	11
215	SO2 adsorption and conversion on pristine and defected calcite {1 0 4} surface: A density functional theory study. Applied Surface Science, 2022, 596, 153575.	3.1	11
216	Strain Energies Due to Nonplanar Distortion of Fullerenes and Their Dependence on Structural Motifs. Journal of Physical Chemistry B, 2006, 110, 218-221.	1.2	10

#	Article	IF	CITATIONS
217	Morphological evolution and electronic alteration of ZnO nanomaterials induced by Ni/Fe co-doping. Nanoscale, 2014, 6, 7312-7318.	2.8	10
218	Synthesis of a Novel Catalyst MnO/CNTs for Microwave-Induced Degradation of Tetracycline. Catalysts, 2019, 9, 911.	1.6	10
219	Single-source precursor synthesis of nitrogen-doped porous carbon for high-performance electrocatalytic ORR application. Ceramics International, 2019, 45, 8354-8361.	2.3	10
220	Learning from nature: Understanding hydrogenase enzyme using computational approach. Wiley Interdisciplinary Reviews: Computational Molecular Science, 2020, 10, e1422.	6.2	10
221	FeCoNi Ternary Spinel Oxides Nanosheets as High Performance Water Oxidation Electrocatalyst. ChemCatChem, 2020, 12, 2209-2214.	1.8	10
222	Evaluation of electrocatalytic dinitrogen reduction performance on diamond carbon via density functional theory. Diamond and Related Materials, 2021, 111, 108210.	1.8	10
223	Computational analysis of apatite-type compounds for band gap engineering: DFT calculations and structure prediction using tetrahedral substitution. Rare Metals, 2021, 40, 3694-3700.	3.6	10
224	Defective 2D silicon phosphide monolayers for the nitrogen reduction reaction: a DFT study. Nanoscale, 2022, 14, 5782-5793.	2.8	10
225	Nanoscale Gd ₂ O ₂ S:Tb Scintillators for High-Resolution Fluorescent Imaging of Cold Neutrons. ACS Applied Nano Materials, 2022, 5, 8440-8447.	2.4	10
226	First Principle Study of Hydrogenation of MgB ₂ : An Important Step Toward Reversible Hydrogen Storage in the Coupled LiBH ₄ /MgH ₂ System. Journal of Nanoscience and Nanotechnology, 2009, 9, 4388-4391.	0.9	9
227	Surface concentration dependent structures of iodine on Pd(110). Journal of Chemical Physics, 2012, 137, 204703.	1.2	9
228	Microstructure evolution and oxidation states of Co in perovskite-type oxide Ba10Co0.7Fe0.2Nb0.1O3– annealed in CO2 atmosphere. Journal of Energy Chemistry, 2014, 23, 575-581.	7.1	9
229	Electronics, Vacancies, Optical Properties, and Band Engineering of Red Photocatalyst SrNbO ₃ : A Computational Investigation. Journal of Physical Chemistry C, 2014, 118, 11267-11270.	1.5	9
230	Comparison of the effect of hydrogen incorporation and oxygen vacancies on the properties of anatase TiO2: electronics, optical absorption, and interaction with water. Science Bulletin, 2014, 59, 2175-2180.	1.7	9
231	Synthesis of Polydopamine Hollow Capsules via a Polydopamine Mediated Silica Water Dissolution Process and Its Application for Enzyme Encapsulation. Frontiers in Chemistry, 2019, 7, 468.	1.8	9
232	Trace-Level Fluorination of Mesoporous TiO ₂ Improves Photocatalytic and Pb(II) Adsorbent Performances. Inorganic Chemistry, 2020, 59, 17631-17637.	1.9	9
233	Computational Investigation of MgH ₂ /NbOx for Hydrogen Storage. Journal of Physical Chemistry C, 2021, 125, 8862-8868.	1.5	9
234	CO ₂ reduction to CH ₄ on Cu-doped phosphorene: a first-principles study. Nanoscale, 2021, 13, 20541-20549.	2.8	9

#	Article	IF	CITATIONS
235	Improved visible light absorption of HTaWO6 induced by nitrogen doping: An experimental and theoretical study. Chemical Physics Letters, 2011, 501, 427-430.	1.2	8
236	The migration behavior of sulfur impurity contained in the dual-phase membrane of Ce0.9Gd0.1O2â~Îr–SrCo0.8Fe0.1Nb0.1O3â~δunder CO2 atmosphere. Journal of Membrane Science, 2016, 51 162-169.	l,4.1	8
237	Confined Synthesis: From Layered Titanate to Highly Efficient and Durable Mesoporous Cu/TiO ₂ Hydrogen Evolution Photocatalysts. ACS Applied Energy Materials, 2021, 4, 4050-4058.	2.5	8
238	A self-similar array model of single-walled carbon nanotubes. Applied Physics Letters, 2005, 86, 203106.	1.5	7
239	Effects of resonance energy and nonplanar strain energy on the reliability of hyperhomodesmotic reactions for corannulene. Chemical Physics Letters, 2007, 434, 160-164.	1.2	7
240	Formation energies of low-indexed surfaces of tin dioxide terminated by nonmetals. Solid State Communications, 2010, 150, 957-960.	0.9	7
241	Adsorption and Dissociation of Ammonia Borane Outside and Inside Single-Walled Carbon Nanotubes: A Density Functional Theory Study. Journal of Physical Chemistry C, 2011, 115, 12580-12585.	1.5	7
242	Computational prediction of hydrogen sulfide and methane separation at room temperature by anatase titanium dioxide. Chemical Physics Letters, 2013, 557, 106-109.	1.2	7
243	Non uniform shrinkages of double-walled carbon nanotube as induced by electron beam irradiation. Applied Physics Letters, 2014, 105, 093103.	1.5	7
244	The oxygen reduction reaction on [NiFe] hydrogenases. Physical Chemistry Chemical Physics, 2018, 20, 23528-23534.	1.3	7
245	Enhanced activity of mesoporous SrCo0.8Fe0.1Nb0.1O3-δ perovskite electrocatalyst by H2O2 treatment for oxygen evolution reaction. Journal of Electroanalytical Chemistry, 2019, 854, 113556.	1.9	7
246	Study on the fluorescence properties of micron-submicron-nano BaFBr:Eu2+ phosphors. New Journal of Chemistry, 2020, 44, 13118-13124.	1.4	7
247	A synergetic effect between a single Cu site and S vacancy on an MoS ₂ basal plane for methanol synthesis from syngas. Catalysis Science and Technology, 2021, 11, 3261-3269.	2.1	7
248	Theoretical investigation of novel p-block metal-based electrocatalysts for nitrogen reduction reaction. Applied Surface Science, 2022, 572, 151441.	3.1	7
249	Boosting nitrogen reduction on single Mo atom by tuning its coordination environment. Sustainable Energy and Fuels, 2021, 5, 6488-6497.	2.5	7
250	The hydrogen storage performance and catalytic mechanism of the MgH2-MoS2 composite. Journal of Magnesium and Alloys, 2023, 11, 2530-2540.	5.5	7
251	Synergistic Effects of B/N Doping on the Visibleâ€Light Photocatalytic Activity of Mesoporous TiO ₂ . Angewandte Chemie - International Edition, 2008, 47, 5277-5277.	7.2	6
252	Visible-light photoresponsive heterojunctions of (Nb–Ti–Si) and (Bi/Bi-O) nanoparticles. Electrochemistry Communications, 2009, 11, 509-514.	2.3	6

#	Article	IF	CITATIONS
253	A Study on the Degradation and Recovery Mechanisms of Perovskite Ba1.0Co0.7Fe0.2Nb0.1O3-δ Membrane Under CO2-Containing Atmosphere. Journal of Physical Chemistry C, 2015, 119, 24229-24237.	1.5	6
254	Iron-doping effects on the CO2 tolerance of a perovskite oxygen permeable membrane. Journal of Materials Science, 2016, 51, 3971-3978.	1.7	6
255	Fabrication and characterization of bulk nanoporous Cu with hierarchical pore structure. Journal of Materials Science, 2017, 52, 12445-12454.	1.7	6
256	First-principles study of the interactions of hydrogen with low-index surfaces of PdCu ordered alloy. Progress in Natural Science: Materials International, 2017, 27, 709-713.	1.8	6
257	Hydrogen Evolution in [NiFe] Hydrogenases: A Case of Heterolytic Approach between Proton and Hydride. Inorganic Chemistry, 2019, 58, 2979-2986.	1.9	6
258	Designed synthesis of ZnO/PEDOT core/shell hybrid nanotube arrays with enhanced electrochromic properties. Surface and Interface Analysis, 2020, 52, 389-395.	0.8	6
259	Exploring adsorption mechanism of glyphosate on pristine and elemental doped graphene. Chemical Physics Letters, 2021, 779, 138849.	1.2	6
260	Selective bimetallic sites supported on graphene as a promising catalyst for CO2 Reduction: A first-principles study. Applied Surface Science, 2022, 582, 152472.	3.1	6
261	Facile synthesis of self support Fe doped Ni3S2 nanosheet arrays for high performance alkaline oxygen evolution. Journal of Electroanalytical Chemistry, 2022, 907, 116047.	1.9	6
262	Continuous g-C ₃ N ₄ layer-coated porous TiO ₂ fibers with enhanced photocatalytic activity toward H ₂ evolution and dye degradation. RSC Advances, 2022, 12, 10258-10266.	1.7	6
263	Amorphous Boron Carbide on Titanium Dioxide Nanobelt Arrays for Highâ€Efficiency Electrocatalytic NO Reduction to NH ₃ . Angewandte Chemie, 0, , .	1.6	6
264	Spectroscopic investigations and density functional theory calculations reveal differences in retention mechanisms of lead and copper on chemically-modified phytolith-rich biochars. Chemosphere, 2022, 301, 134590.	4.2	6
265	Packing-dependent pore structures in single-walled carbon nanotube arrays. Applied Physics Letters, 2005, 87, 243109.	1.5	5
266	Influence of High-Temperature Water Vapor on Titanium Film Surface. Oxidation of Metals, 2016, 86, 179-192.	1.0	5
267	Silver Molecularly Imprinting Polymer for the Determination of p-Nitroaniline by Surface Enhanced Raman Scattering. Analytical Letters, 2019, 52, 1888-1899.	1.0	5
268	CO activation and methanation mechanism on hexagonal close-packed Co catalysts: effect of functionals, carbon deposition and surface structure. Catalysis Science and Technology, 2020, 10, 3387-3398.	2.1	5
269	A novel cobalt-free and CO ₂ -stable LDC-LSCF membrane with high oxygen permeability. Surface Innovations, 2022, 10, 59-67.	1.4	5
270	Superior electrocatalytic ORR performance of Melaleuca Leucadendron L barks derived hierarchical porous carbon with abundant atom-scale vacancies and multiheteroatoms. Ceramics International, 2022, 48, 11111-11123.	2.3	5

#	Article	IF	CITATIONS
271	Finding Key Factors for Efficient Water and Methanol Activation at Metals, Oxides, MXenes, and Metal/Oxide Interfaces. ACS Catalysis, 2022, 12, 1237-1246.	5.5	5
272	Insight into the Reactivity of Carbon Structures for Nitrogen Reduction Reaction. Langmuir, 2021, 37, 14657-14667.	1.6	5
273	Comparative Studies of Hyperhomodesmotic Reactions for the Calculation of Standard Heats of Formation of Fullerenes. Journal of Physical Chemistry A, 2006, 110, 299-302.	1.1	4
274	Theoretical study of K3Sb/graphene heterostructure for electrochemical nitrogen reduction reaction. Frontiers of Physics, 2022, 17, 1.	2.4	4
275	Size-Dependent Nonlinear Optical Properties of Gd2O2S:Tb3+ Scintillators and Their Doped Gel Glasses. Molecules, 2022, 27, 85.	1.7	4
276	Fractal effects on the measurement of the specific surface areas of single-walled carbon nanotubes. Carbon, 2005, 43, 1785-1787.	5.4	3
277	Half metallicity in a zigzag double-walled nanotube nanodot: An ab initio prediction. Chemical Physics Letters, 2009, 468, 257-259.	1.2	3
278	Enhanced performance of organic light-emitting devices by using electropolymerized poly(3,4-ethylenedioxythiophene):poly(styrene sulfonate) film as the anode modification layer. Thin Solid Films, 2012, 520, 2979-2983.	0.8	3
279	Controllable fabrication of bulk hierarchical nanoporous palladium by chemical dealloying at various temperature and its thermal coarsening. Journal of Porous Materials, 2018, 25, 555-563.	1.3	3
280	Effect of Spark Plasma Sintering on the Structure and Compressive Strength of Porous Nickel. Powder Metallurgy and Metal Ceramics, 2018, 57, 154-160.	0.4	3
281	Density functional theory study of perfluorooctane sulfonate adsorption on fluorinated graphene. Surface Innovations, 2021, 9, 149-155.	1.4	3
282	Nâ€Doped CsTaWO ₆ as a New Photocatalyst for Hydrogen Production from Water Splitting Under Solar Irradiation. Advanced Functional Materials, 2011, 21, 125-125.	7.8	2
283	Fabrication, characterization and electrochemical properties of porous palladium bulk samples with high porosity and hierarchical pore structure. Chinese Journal of Catalysis, 2017, 38, 1038-1044.	6.9	2
284	Characterization and Thermal Stability Properties of Bulk Hierarchical Porous Pd Prepared by Kirkendall Effect and Dealloying Method. Journal of Nanomaterials, 2018, 2018, 1-7.	1.5	2
285	Design of heterojunction with components in different dimensions for electrocatalysis applications. Frontiers of Physics, 2022, 17, .	2.4	2
286	Estimation of Standard Heats of Formation of Fullerenes Using Pentagon-Centered Motifs. Journal of Physical Chemistry C, 2007, 111, 18503-18506.	1.5	1
287	Standard enthalpies of formation of finite-length (5, 5) single-walled carbon nanotube. Journal of Nanoparticle Research, 2008, 10, 1037-1043.	0.8	1
288	Chapter 6. DFT Modelling Tools in CO2 Conversion: Reaction Mechanism Screening and Analysis. RSC Energy and Environment Series, 2018, , 136-159.	0.2	1

#	Article	IF	CITATIONS
289	Effect of local coordination on catalytic activities and selectivities of Fe-based catalysts for N ₂ reduction. Physical Chemistry Chemical Physics, 2022, 24, 14517-14524.	1.3	1
290	Moâ€Doped Sulfurâ€Vacancyâ€Rich V _{1.11} S ₂ Nanosheets for Efficient Hydrogen Evolution. ChemistrySelect, 2022, 7, .	0.7	1
291	Photocatalysis: Constructing a Metallic/Semiconducting TaB2/Ta2O5Core/Shell Heterostructure for Photocatalytic Hydrogen Evolution (Adv. Energy Mater. 12/2014). Advanced Energy Materials, 2014, 4, n/a-n/a.	10.2	0
292	Computational investigation of the co-doping effect of sulphur andÂnitrogen on the electronics of CsTaWO 6. Journal of Materiomics, 2017, 3, 71-76.	2.8	0
293	Operando Metalloid Znδ+ Active Sites for Highly Efficient Carbon Dioxide Reduction Electrocatalysis. Angewandte Chemie, 0, , .	1.6	0